

DOI: 10.17725/rensit.2023.15.169

## Holographic processing of hydroacoustic information using linear antennas

**Venedikt M. Kuz'kin**

Prokhorov Institute of General Physics of Russian Academy of Sciences, <http://www.gpi.ru/>  
Moscow 119991, Russian Federation

*E-mail: kumiov@yandex.ru*

**Sergey A. Pereselkov, Sergey A. Tkachenko, Nadezhda P. Stadnaya**

Voronezh State University, <http://www.vsu.ru/>

Voronezh 394006, Russian Federation

*E-mail: pereselkov@yandex.ru; sega-th@mail.ru, stadnaya.edu@yandex.ru*

**Yuri V. Matvienko**

Institute for Marine Technology Problems, Far Eastern Branch of Russian Academy of Sciences, <http://www.febras.ru/>

Vladivostok 690091, Russian Federation

*E-mail: ymat@marine.febras.ru*

**Vladimir I. Grachev**

Kotelnikov Institute of Radioengineering and Electronics of RAS, <http://www.cplire.ru/>

Moscow 125009, Russian Federation

*E-mail: grachev@cplire.ru*

*Received May 25, 2023, peer-reviewed May 31, 2023, accepted June 07, 2023*

**Abstract:** The formation of an interferogram and a hologram of a moving underwater noise source using linear antennas is considered. The relationship between the spectral density of the hologram and the aperture and the angular dependence of the received field is derived. Antenna gain has been estimated. The issue of the limiting signal-to-noise ratio at which the holographic processing remains operational is discussed. An analytical expression is obtained that establishes a relationship between the signal/noise ratios at the output and input of the antenna. Conditions are formulated under which the interferogram of the source is not distorted.

**Keywords:** shallow water area, interferogram, hologram, noise source, linear antenna, signal-to-noise ratio, antenna parameters

**UDC 004.052.34**

**Acknowledgments:** The study was supported by the Russian Science Foundation grant No. 23-61-10024, <https://rscf.ru/project/23-61-10024/>. Numerical calculations of antenna parameters S.A. Tkachenko were supported by the grant of the Russian Federation President MK-4846.2022.4.

**For citation:** Venedikt M. Kuz'kin, Sergey A. Pereselkov, Yuri V. Matvienko, Vladimir I. Grachev, Sergey A. Tkachenko, Nadezhda P. Stadnaya. Holographic processing of hydroacoustic information using linear antennas. *RENSIT: Radioelectronics. Nanosystems. Information Technologies*, 2023, 15(2):169-178e. DOI: 10.17725/rensit.2023.15.169.

### CONTENTS

- |  |  |
|--|--|
| <p>1. INTRODUCTION (170)</p> <p>2. HOLOGRAPHIC PROCESSING USING LINEAR ANTENNAS (170)</p> <p>    2.1. HORIZONTAL LINE ANTENNA (171)</p> <p>    2.2. VERTICAL LINE ANTENNA (172)</p> <p>3. ANTENNA PARAMETERS (172)</p> | <p>3.1. Amplification factor and directivity characteristic (172)</p> <p>3.2. LIMIT INPUT SIGNAL-TO-NOISE RATIO (173)</p> <p>3.3. NOISE IMMUNITY (173)</p> <p>4. CRITERIA FOR THE FORMATION OF AN UNDISTORTED INTERFEROGRAM (175)</p> <p>5. CONCLUSION (176)</p> <p>REFERENCES (177)</p> |
|--|--|

## 1. INTRODUCTION

Currently, one of the topical areas of underwater research is the illumination of the underwater environment, which ensures the detection and localization (resolution, determination of bearing, radial velocity, distance and depth) of moving underwater low-noise sound sources using small-sized antennas. The solution to this problem based on holographic processing based on stable structural features of the interference pattern (interferogram) formed by a noise source is considered in [1–3]. Interferogram refers to the energy characteristics of the received vector-scalar field in frequency-time variables. Holographic processing implements quasi-coherent accumulation of the spectral density of a noise source along localized interferogram fringes in frequency-time variables. During the observation time  $\Delta t$ , in the band  $\Delta f$ ,  $J$  independent realizations are accumulated with duration  $t_1$  and with a time interval  $t_2$  between them

$$J = \frac{\Delta t}{t_1 + t_2}. \quad (1)$$

Realizations are independent if  $t_2 > 1/\Delta f$ . Noise accumulation is incoherent. An interferogram is formed in frequency-time variables, to which a two-dimensional Fourier transform is applied. At the output of the integral transformation (hologram), the spectral density is concentrated in a narrow band in the form of focal spots caused by the interference of modes of different numbers. The spectral density of interference is distributed over the entire region. Such processing has a high noise immunity. Based on the location of the spectral densities of holograms and some a priori data on the propagation channel, the problems of detection, direction finding, determination of the radial velocity, distance and resolution of sources are solved.

Holographic processing today is a very active field of research, in which many interesting results of theoretical and practical interest have been obtained. First, a method has been developed for restoring the interferogram of an unperturbed field on a stationary path, when intense internal waves cause horizontal refraction and interaction of acoustic field modes [4–7]. Secondly, a noise-resistant method for detecting and localizing moving low-noise sources, which is stable with respect to the hydrodynamic variability of the oceanic environment, has been proposed [8]. Thirdly, adaptive algorithms for determining the source parameters have been created that do not require knowledge about the characteristics of the propagation medium [9,10]. Further, fourthly, a method is implemented for resolving several sources of different intensities under conditions when their interferograms overlap in frequency and time and are masked by interference [11]. Finally, fifthly, a method has been developed for selecting acoustic field modes and determining their parameters [12–14]. Works [15–18] have played a significant role in the progress in the development of holographic interferometry in shallow water areas.

The purpose of this article is, firstly, to describe holographic processing using linear antennas and consider their characteristics that determine the effectiveness of the work. Secondly, to reveal the reception conditions under which the interferogram of the source is not distorted in the absence of interference.

## 2. HOLOGRAPHIC PROCESSING USING LINEAR ANTENNAS

Let the number of elements  $Q_b$  of the receiving antenna be equal to  $B$ ,  $b = \overline{1, B}$ , the interelement distance is  $d$ . The received

spectrum of a noise source moving with a radial velocity  $w$  at a depth  $z_s$  is concentrated in the frequency range  $f_1 \leq f \leq f_2$ , where  $f_{1,2} = f_0 \pm (\Delta f/2)$ ,  $\Delta f$  and  $f_0$  are the bandwidth and the average frequency of the spectrum. The fields from each antenna element are summed, and an interferogram is formed at the output, to which a two-dimensional Fourier transform is applied. We will consider the processing using the example of the scalar component of the field, i.e. sound pressure spectrum  $p(f, t)$ .

2.1. HORIZONTAL LINE ANTENNA

The layout of the source  $S$  and the horizontal linear antenna is shown in Fig. 1. The antenna elements are at a depth  $z_q$ . The reference element of the antenna is the first element  $Q_1$ . The aperture  $L = (B - 1)d$  is much smaller than the distance to the source. In this case,  $r_b = r_1 - (b - 1)d \sin \theta$ , where  $\theta$  is the angle complementary to the bearing.

When summing the fields from the antenna elements, the difference in distances from the source to its various elements in the direction of the angle  $\theta$  is compensated. Therefore, the field  $Q_b$  of the element is multiplied by the exponential factor  $\exp[ih_*(f_0)(b - 1)d \sin \theta]$ . Here  $h_*(f_0)$  is the distinguished real part of the horizontal

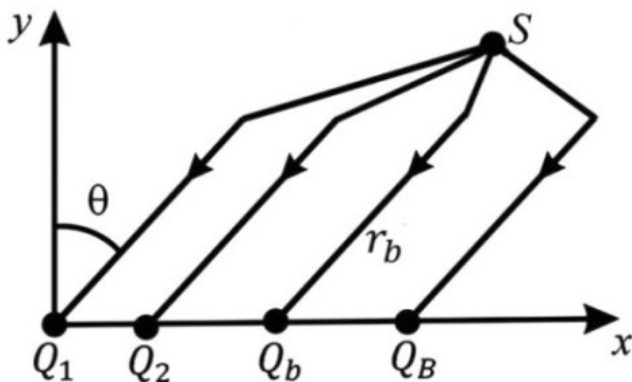


Fig. 1. Geometry of the problem (view in the horizontal plane):  $r_b$  is the horizontal distance of the element  $Q_b$  to the source  $S$ ,  $\theta$  is the angle of direction to the source.

wavenumber (propagation constant) at the middle frequency  $f_0$  of the source spectrum,  $\theta_*$  is the compensation angle. The field at the output  $Q_b$  of the antenna element can be represented as a sum of modes [19]

$$p_b(f, r_b) = \sum_m A_m(f, r_b) \exp\{i[h_m(f)r_1 - 2(b-1)(h_m(f) - h_*(f_0)_*)]\}, \tag{2}$$

where

$$\eta = d \sin \theta / 2, \eta_* = d \sin \theta_* / 2. \tag{3}$$

Here  $A_m$  and  $h_m$  are the amplitude and propagation constant of the  $m$ -mode. Cylindrical field divergence, modal attenuation, source depths  $z_s$  and antenna element depths  $z_b$  are taken into account in the modal amplitude. At the antenna output, the field  $p_{an}(f, r_1)$ , neglecting the dependence of the amplitude on distance,  $A_m(f, r_1) \approx A_m(f, r_b)$ , we write as

$$p_{an}(f, r_1) = \sum_m A_m(f, r_1) I_m \exp\{i[h_m(f)r_1 - (B-1)(h_m(f)\eta - h_*(f_0)\eta_*)]\}, \tag{4}$$

where

$$I_m(f) = \frac{\sin[B(h_m(f)\eta - h_*(f_0)\eta_*)]}{\sin(h_m(f)\eta - h_*(f_0)\eta_*)}. \tag{5}$$

The antenna interferogram  $P_{an}(f, r_1) = |p_{an}(f, r_1)|^2$ , according to (4), is equal to

$$P_{an}(f, r_1) = \sum_m \sum_n P_{an}^{(mn)}(f, r_1), \tag{6}$$

$$P_{an}^{(mn)}(f, r_1) = A_m(f, r_1) A_n^*(f, r_1) I_{mn}(f) \times \exp[ih_{mn}(f)(r_1 - (B-1)\eta)], \tag{7}$$

where

$$I_{mn}(f) = I_m(f) I_n^*(f). \tag{8}$$

Here  $h_{mn}(f) = h_m(f) - h_n(f)$ . Let at the initial time  $t_0 = 0$  the distance  $r_1 = r_0$ . In interferogram (6), we pass from the distance variable  $r_1$  to the time variable  $t$ ,  $r_1 = r_0 + wt$ , and apply the two-dimensional Fourier transform to it.

At the output of the integral transformation (hologram), the spectral density is expressed through the interferogram as

$$F_{an}(v, \tau) = 2\pi \int_0^{\Delta t} \int_{f_1}^{f_2} P_{an}(f, t) \exp[i2\pi(vt - f\tau)] dt df =$$

$$= \sum_m \sum_n F_{an}^{(mn)}(v, \tau), \quad (9)$$

where  $v$  and  $\tau$  are the frequency and time of the hologram;  $\Delta t$  is the observation time. Using the approach for calculating the hologram of a single receiver [1], for partial antenna holograms, we obtain

$$F_{an}^{(mn)}(v, \tau) = 2\pi A_m(f_0, r_0) A_n^*(f_0, r_0) I_{mn}(f_0) \Delta f \Delta t \times$$

$$\times \exp\left[i2\pi\left(\frac{v\Delta t}{2} - \tau f_0\right)\right] \times$$

$$\times \exp\left\{i\left[h_{mn}(f_0)\left(\frac{w\Delta t}{2} + r - (B-1)\eta\right)\right]\right\} \times$$

$$\sin\left\{\pi\left[\left(r_0 - (B-1)\eta + wt_*\right) \frac{1}{2\pi} \frac{dh_{mn}(f_0)}{df} - \tau\right] \Delta f\right\} \quad (10)$$

$$\times \frac{\pi\left[\left(r_0 - (B-1)\eta + wt_*\right) \frac{1}{2\pi} \frac{dh_{mn}(f_0)}{df} - \tau\right] \Delta f}{\pi\left[\left(r_0 - (B-1)\eta + wt_*\right) \frac{1}{2\pi} \frac{dh_{mn}(f_0)}{df} - \tau\right] \Delta f}$$

$$\times \frac{\sin\left\{[wh_{mn}(f_0) + 2\pi v] \frac{\Delta t}{2}\right\}}{[wh_{mn}(f_0) + 2\pi v] \frac{\Delta t}{2}}.$$

Here  $t_*$  is the distinguished moment of time on the observation interval  $\Delta t$ ,  $0 < t_* < \Delta t$ . If we set  $B = 1$ , then  $I_{mn}(f_0) = 1$  and formula (10) becomes the corresponding formula for a single receiver [1]. The factor  $I_{mn}(f_0)$  (8) determines the distribution of the spectral density of the antenna hologram with respect to a single receiver. The dependences of  $I_{mn}(f_0)$  on the angle  $\theta$  at the compensation angle  $\theta_* = 0$  are considered in [20].

## 2.2. VERTICAL LINE ANTENNA

The field at the output of the  $b$ -th element at a horizontal distance  $r$  from the noise source is written as a sum of modes as [19]

$$p_b(f, r, z_b) = \sum_m \psi_m(z_b) A_m(f, r) \exp[ih_m(f)r], \quad (11)$$

where  $\psi_m(z)$  – eigenfunction of the  $m$ th mode. In (11), the slow change in the eigenfunction with frequency is neglected. At the output of the antenna, the source field takes the form

$$p_{an}(f, r) = \sum_b p_b(f, r) = \sum_m E_m A_m(f, r) \exp[ih_m(f)r], \quad (12)$$

where

$$E_m = \sum_n \psi_n(z_b). \quad (13)$$

The antenna interferogram, according to (12), is equal to

$$P_{an}(f, r) = \sum_m \sum_n P_{mn}(f, r), \quad (14)$$

$$P_{mn}(f, r) = E_m E_n^* A_m(f, r) A_n^*(f, r) \exp[ih_{mn}(f)r]. \quad (15)$$

Let the initial time  $t_0 = 0$  correspond to the distance  $r_0$ . In the interferogram (14), we pass from the distance variable  $r$  to the time variable  $t$  and apply the two-dimensional Fourier transform (9) to it. As a result, for partial antenna holograms, we obtain

$$F_{an}^{(mn)}(v, \tau) = 2\pi A_m(f_0, r_0) A_n^*(f_0, r_0) E_m E_n^* \Delta f \Delta t \times$$

$$\times \exp\left[i2\pi\left(\frac{v\Delta t}{2} - \tau f_0\right)\right] \exp\left[ih_{mn}(f_0)\left(\frac{w\Delta t}{2} + r_0\right)\right] \times$$

$$\sin\left\{\pi\left[\left(r_0 + wt_*\right) \frac{1}{2\pi} \frac{dh_{mn}(f_0)}{df} - \tau\right] \Delta f\right\}$$

$$\times \frac{\pi\left[\left(r_0 + wt_*\right) \frac{1}{2\pi} \frac{dh_{mn}(f_0)}{df} - \tau\right] \Delta f}{\pi\left[\left(r_0 + wt_*\right) \frac{1}{2\pi} \frac{dh_{mn}(f_0)}{df} - \tau\right] \Delta f} \quad (16)$$

$$\times \frac{\sin\left\{[wh_{mn}(f_0) + 2\pi v] \frac{\Delta t}{2}\right\}}{[wh_{mn}(f_0) + 2\pi v] \frac{\Delta t}{2}}.$$

If we put  $B = 1$ , then relation (16) turns into an expression for a single receiver [1]. The spectral density of the partial holograms of the antenna  $F_{an}^{(mn)}$  with respect to a single receiver differs by a weight factor  $E_m E_n^*$ . For this reason, the regions of localization of the spectral density for the antenna and a single receiver are similar in shape.

## 3. ANTENNA PARAMETERS

### 3.1. AMPLIFICATION FACTOR AND DIRECTIVITY CHARACTERISTIC

The effectiveness of holographic processing using receiving antennas characterizes the amplification factor

$$\chi = G_{an} / G_r \quad (17)$$

and directivity characteristic (horizontal antenna)

$$D = G_{an} / \max G_{an}, \quad (18)$$

where

$$G_{an,r} = \iint |F_{an,r}(\tau, \nu)| d\tau d\nu. \quad (19)$$

Index "r" refers to a single receiver. In the compensation angle direction, the amplification factor of horizontal antenna reaches its maximum value  $\chi_{max} \cong B^2$ . The amplification factor  $\chi$  of the vertical antenna is  $\chi \approx B^2$ . Thus, the amplification factors of the horizontal and vertical antennas are comparable to each other. The results of numerical simulation for considering the amplification factor and directivity characteristics of linear antennas were discussed in [20, 21].

### 3.2. LIMIT INPUT SIGNAL-TO-NOISE RATIO

Holographic processing has certain limitations, which lie in the nature of interference phenomena and the presence of interference. The restriction associated with interference can be conveniently characterized by the limiting (minimum) input signal-to-noise ratio (s/n)  $q_{lim}$ , when stable detection and estimates of bearing, radial velocity, distance, and depth are close to real for input s/n  $q_0 > q_{lim}$ . In the case of isotropic interference and a single receiver for the scalar component of the noise source field  $q_{lim}^{(r)} \approx 1.5/f^2$  [2]. The estimate was established on the basis of a number of physical considerations and verified on the results of numerical and natural experiments. When using the combinational components of the vector-scalar field, the value  $q_{lim}^{(r)}$  decreases by 2-5 times [2,3]. Let us generalize the estimate of the limiting input s/n ratio of a single receiver to linear antennas.

Let us assume that the noise signal and interference are statistically unrelated random processes and the interference at the input of the antenna elements is not correlated. The second condition is satisfied if  $d \geq \lambda/2$ , where  $\lambda$  is the wavelength. Then the limit input s/n ratio on the antenna element is estimated as

$$q_{lim}^{(an)} = \alpha q_{lim}^{(r)}, \quad (20)$$

where  $\alpha = B/\chi$ . The value of  $\chi \approx B^2$ , so  $\alpha \approx 1/B$ . The input s/n ratios on a single antenna element, when the estimates of the source parameters are close to real values, are limited by the inequality  $q_0 > q_{lim}^{(an)}$ . If, first, holographic processing is performed on each  $b$ -th receiver and then the spectral densities of the holograms are summed at the antenna output, then there will be no gain in the limiting s/n ratio with respect to a single receiver.

### 3.3. NOISE IMMUNITY

Let us consider how the s/n ratio at the antenna output is related  $q_{an}^{(out)}$  to the s/n ratio at the input of the antenna element  $q_0$ . Their ratio, as is known, determines the noise immunity of processing

$$\rho_{an} = \frac{q_{an}^{(out)}}{q_0}. \quad (21)$$

When solving this problem, we first analyze the question of the relationship between the s/n ratios  $q_r^{(out)}$  at the output and input  $q_0$  of a single receiver.

Let the pressure spectra of the noise signal and interference, which we denote as  $s(t, f)$  and  $n(t, f)$ , be concentrated in the band  $\Delta f$ . Signal and noise are mutually independent Gaussian random stationary processes with zero mathematical expectations. We restrict ourselves to  $q_0$  values satisfying the condition  $q_0 > q_{lim}^{(r)}$ . Let us assume that the band  $\Delta f$  contains  $W$  localized bands of width  $\delta f$  and the contrast of the interferogram, i.e. the bands visibility is equal to one. Let us assume that the noise signal field accumulates coherently along the interference fringes, while interferences accumulates incoherently. Strictly speaking, this provision is not fulfilled, however, from the qualitative and quantitative side, as shown by the data of computer simulation and field experiments [1-3,11], the results remain quite meaningful.

The s/n ratio  $q_0$  at the input of a single receiver at the initial time  $t = 0$  is understood as the value

$$q_0 = q(0) = \frac{\overline{E_s(0)}}{\overline{E_n(0)}}, \quad (22)$$

where

$$\overline{E_s(0)} = 2 \int_0^\infty \overline{|s(0, f)|^2} df = 2 \Delta f \overline{|s(0, f_s')|^2}, \quad (23)$$

$$\overline{E_n(0)} = 2 \int_0^\infty \overline{|n(0, f)|^2} df = 2 \Delta f \overline{|n(0, f_n')|^2}, \quad (24)$$

– average signal energies and interference. Here  $f_s'$  and  $f_n'$  are the selected signal frequencies and noise in the band  $\Delta f$ . The overline means averaging over the ensemble of realizations. In accordance with (23), (24), the input ratio s/n (22) is equal to

$$q_0 = \frac{\overline{|s(0, f_s')|^2}}{\overline{|n(0, f_n')|^2}}. \quad (25)$$

The average signal energies and noise at the output of trajectory accumulation over time  $\Delta t$  can be written in the form of summation of energies over time intervals of duration  $t_1$  along the interference fringes

$$\overline{E_s(\Delta t)} = 2 \int_0^\infty \left| \sum_{j=1}^J W s(t_j, f) \right|^2 df, \quad (26)$$

$$\overline{E_n(\Delta t)} = 2 W J \sum_{j=1}^J \int_0^\infty \overline{|n(t_j, f)|^2} df. \quad (27)$$

Using the assumption of stationarity of processes, expressions (26), (27) can be reduced to the form

$$\overline{E_s(\Delta t)} = 2 W^2 J^2 \overline{|s(f_s'')|^2} \delta f, \quad (28)$$

$$\overline{E_n(\Delta t)} = 2 W J \overline{|n(f_n'')|^2} \delta f, \quad (29)$$

so that at the output of the trajectory accumulation, the ratio s/n is equal to

$$q_r(\Delta t) = \frac{\overline{E_s(\Delta t)}}{\overline{E_n(\Delta t)}} = W J \frac{\overline{|s(f_s'')|^2}}{\overline{|n(f_n'')|^2}}. \quad (30)$$

Here  $f_s''$  and  $f_n''$  – selected signal frequencies and interference in the band  $\delta f$ .

Using the input ratio s/n (25), we represent expression (30) in the form

$$q_r(\Delta t) = J W \frac{\overline{|s(f_s'')|^2} \overline{|n(f_n'')|^2}}{\overline{|n(f_n'')|^2} \overline{|s(f_s'')|^2}} q_0. \quad (31)$$

At the initial moment of time, the average energies of the signal (23) and interference (24) can also be expressed as

$$\overline{E_s(0)} = 2 W^2 \overline{|s(f_s'')|^2} \delta f, \quad (32)$$

$$\overline{E_n(0)} = 2 W \overline{|n(f_n'')|^2} \delta f. \quad (33)$$

From a comparison of expressions (23), (24) and (32), (33) we find

$$\overline{|s(f_s'')|^2} \Delta f_1 = W \overline{|s(f_s'')|^2} \Delta f_2, \quad (34)$$

$$\overline{|n(f_n'')|^2} \Delta f_1 = W \overline{|n(f_n'')|^2} \Delta f_2. \quad (35)$$

and then expression (32) takes the form

$$q_r(\Delta t) = J q_0, \quad (36)$$

so that at the output of trajectory accumulation, the s/n ratio does not depend on the number of interference fringes  $W$  and their width  $\delta f$ , and is proportional to the input s/n ratio  $q_0$  up to a factor  $J$ .

Thus, the multiple coherent summation of the interference maxima of the wave field of the noise source along the localized fringes increases the output s/n ratio  $q_r(\Delta t)$  by a factor of  $J$  with respect to the input value  $q_0$ . Such an increase becomes clear if we draw an analogy with the coherent spatial processing of a multi-element antenna containing  $J$  receivers: with respect to a single receiver, the s/n ratio increases by a factor of  $J$ .

Recording an interferogram onto a hologram and clearing the region of spectral density localization from interference leads to an additional increase in the output s/n ratio compared to  $q_r(\Delta t)$ . The two-dimensional Fourier transform of the interferogram

localizes the two-dimensional spectral density of the noise signal within a narrow band of the hologram, the area of which can be estimated as

$$S_s = \frac{\tau_*}{\Delta t}. \tag{37}$$

Here  $\tau_*$  is the position of the main maximum of the focal spot on the time axis due to interference between the extreme modes. The spectral noise density is distributed over the entire region of the hologram, the area of which is equal to

$$S_n = |\nu_*| \tau_*, \tag{38}$$

where  $\nu_*$  is the position of the main maximum of the focal spot on the frequency axis due to interference between the extreme modes. During the integral transformation, the energy does not change.

Assuming the interference power to be uniformly distributed in the hologram region, the s/n ratio at the output of holographic processing can be represented as

$$q_r^{(out)} = \gamma q_r(\Delta t), \quad \gamma = S_n / S_s, \tag{39}$$

where the concentration coefficient, according to (37), (38),  $\gamma = |\nu_*| \Delta t$ . In the case of a stationary source, the quantity  $\nu_*$  is replaced by the spectral width  $\Delta\nu$  in the region of the hologram. In accordance with (36), expression (39) takes the form

$$q_r^{(out)} = J\gamma q_0. \tag{40}$$

Thus, the noise immunity of holographic processing using a single receiver is estimated as

$$\rho_r = J\gamma. \tag{41}$$

It is easy to see how the output s/n ratio at the output of the antenna can be estimated. According to (10), (16), the value of the concentration coefficient  $\gamma$  does not change. Taking into account that the noise signal and interference are accumulated coherently and incoherently, the s/n ratio at the antenna output, with respect to a single receiver, increases by

$1/\alpha = \chi/B \approx B$  times. Therefore, the s/n ratio at the output of the antenna will be

$$q_{an}^{(out)} = (J\gamma / \alpha) q_0. \tag{42}$$

#### 4. CRITERIA FOR FORMING AN UNDISTORTED INTERFEROGRAM

The formation of an interferogram, respectively, and a hologram, is affected by background interference, spatio-temporal inhomogeneities of the propagation medium, and reception conditions. At present, the state of the art on the influence of distorting factors on the formation of an interferogram is mainly concentrated on such aspects as interference [1-3] and intense internal waves [4-8].

In this section, we consider the influence of reception conditions – bandwidth and accumulation time – on the formation of an undistorted interferogram in a regular waveguide in the interference absence. Based on the fact that the interference pattern of the sound source is characterized by frequency  $\Lambda_f^{(mn)}$  and time  $\Lambda_t^{(mn)}$  scales of variability due to the interference of the  $m$ -th and  $n$ -th modes [19]

$$\Lambda_f^{(mn)} = \frac{2\pi}{r |dh_{mn}(f_0) / df|}, \quad \Lambda_t^{(mn)} = \frac{1}{|wh_{mn}(f_0)|}, \tag{43}$$

let us establish the following two criteria for the formation of an undistorted interferogram. For any pair of  $(m, n)$  modes:

I. The frequency range  $f_1 \leq f \leq f_2$  should not be less than the frequency period of interferogram variability

$$\Delta f \geq \Lambda_f^{(mn)}. \tag{44}$$

II. The observation time  $\Delta t$  should not be less than the time period of interferogram variability

$$\Delta t \geq \Lambda_t^{(mn)}. \tag{45}$$

Conditions (44), (45) imply certain restrictions on the bandwidth and observation time depending on the distance, radial velocity,

and time-frequency scales of the variability of the transfer function of the medium during the formation of an undistorted interferogram. Reducing the distance and increasing the average frequency of the spectrum leads to the requirement to increase the bandwidth. The latter is due to the fact that, as the frequency increases, the group velocities of the modes  $u_m(\omega_0) = d\omega/dh_m(\omega_0)$  asymptotically tend to a value that does not depend on the mode number [19]. A decrease in the radial velocity and the average frequency of the spectrum cause an increase in the observation time. The criteria are most critical with respect to the numbers of neighboring modes.

Criterion I excludes the possibility of the formation of an interferogram due to the interference of  $(m, n)$  modes with a uniform spectral density, i.e. in a band of infinite width, when localized bands are not observable. It is useful to note that the violation of condition (44) with respect to all pairs of interfering modes leads to a spectral density in the hologram in the form of a single focal spot at the origin. A different situation is observed when condition (45) is not met, when the observation time is not enough for the source to intersect the spatial scales of the variability of the interference pattern. In this case, the position of the peak of the focal spot formed by such interfering modes is shifted to the time axis of the hologram, since the interferogram is formed with respect to them by a stationary source. The formulated conditions (44) and (45) make it possible to estimate the bandwidth and observation time to reduce the error in reconstructing the parameters of a moving noise source.

## 5. CONCLUSION

Holographic processing of hydroacoustic information has made it possible to change the solution of the problem of detection

and localization of moving low-noise underwater noise sources in the most significant way. It turned out to be possible to establish, in the most general case, simple and transparent relationships between the measured characteristics of the spectral density of a hologram and the parameters of a low-noise underwater source. This gave the holographic processing a certain completeness and very tangible advantages compared to other types of processing in solving specific problems of monitoring the underwater situation with a small input noise signal against the background of interference. As a result, a radical simplification of the solution of the problem of detecting and localizing the source of underwater noise has been achieved, and, at the same time, a significant expansion of the range of problems that can be solved in general. For example, with a small input  $s/n$  ratio against the background of space-time inhomogeneities and in the absence of information about the hydroacoustic characteristics of the propagation medium.

The paper presents the theory of holographic processing of hydroacoustic information using linear horizontal and vertical antennas. The structure of interferograms and holograms is considered. Expressions for the gain and directivity characteristics are given. The limiting input ratio  $s/n$  is estimated, above which the parameters of the noise source of the sound are adequately restored. A connection is established between the output and input  $s/n$  relations. The relations obtained allow us to consider a wide range of problems of monitoring the underwater situation using linear antennas. Restrictions on the bandwidth and observation time are formulated, which ensure the minimum error in the reconstructed parameters of the noise source.

## REFERENCES

1. Kuznetsov GN, Kuz'kin VM, Pereselkov SA. Spectrogram and sound source localization in a shallow sea. *Acoustic Journal*, 2017, 63(4):406-418.
2. Kuznetsov GN, Kuz'kin VM, Pereselkov SA, Kaznacheev IV, Grigor'ev VA. Interferometric method for estimating the velocity of a noise sound source and the distance to it in shallow water using a vector-scalar receiver. *Phys. Wave Phenom.*, 2017, 25(4):299-306.
3. Kaznacheev IV, Kuznetsov GN, Kuz'kin VM, Pereselkov SA. Interferometric method for detecting a moving sound source by a vector-scalar receiver. *Acoustic Journal*, 2018, 64(1):33-45.
4. Kuz'kin VM, Pereselkov SA, Zvyagin VG, Malykhin AYu, Prosovetskiy DYu. Intense internal waves and their manifestation in interference patterns of received signals on oceanic shelf. *Phys. Wave Phenom.*, 2018, 26(2):160-167.
5. Badiy M, Kuz'kin VM, Lyakhov GA, Pereselkov SA, Prosovetskiy DYu, Tkachenko SA. Intense internal waves and their manifestation in the interference patterns of received signals on oceanic shelf. Part II. *Phys. Wave Phenom.*, 2019, 27(4):313-319.
6. Kuz'kin VM, Lyakhov GA, Pereselkov SA, Kaznacheeva ES. Transmission of information through a randomly inhomogeneous oceanic medium. *Fundam. appl. hydrof.*, 2021, 14(2):54-64.
7. Kaznacheeva ES, Kuz'kin VM, Pereselkov SA. Interferometric processing of hydroacoustic information in the presence of intense internal waves. *Phys. Wave Phenom.*, 2021, 29(3):278-284.
8. Kuz'kin VM, Pereselkov SA, Kaznacheeva ES, Grachev VI, Tkachenko SA, Rybyanets PV. Holographic processing of moving sources in a shallow sea in the presence of intense internal waves. *RENSIT: Radioelectronics. Nanosystems. Information Technology*, 2022, 14(2):197-204. DOI: 10.17725/rensit.2022.14.197.
9. Kaznacheeva ES, Kuznetsov GN, Kuz'kin VM, Lyakhov GA, Pereselkov SA. Measurement capability of the interferometric method of sound source localization in the absence of data on the waveguide transfer function. *Phys. Wave Phenom.*, 2019, 27(1):73-78.
10. Kaznacheeva ES, Kuz'kin VM, Lyakhov GA, Pereselkov SA, Tkachenko SA. Adaptive algorithms for interferometric processing. *Phys. Wave Phenom.*, 2020, 28(3):267-273.
11. Kuz'kin VM, Kuznetsov GN, Pereselkov SA, Grigor'ev VA. Resolving power of the interferometric method of source localization. *Phys. Wave Phenom.*, 2018, 26(2):150-159.
12. Kuz'kin VM, Matvienko YuV, Pereselkov SA, Prosovetskiy DYu, Kaznacheeva ES. Mode selection in oceanic waveguides. *Phys. Wave Phenom.*, 2022, 30(2):111-118.
13. Kuz'kin VM, Pereselkov SA, Kaznacheeva ES, Grachev VI, Tkachenko SA, Rybyanets PV. Isolation of modes of a noise source in a shallow sea by holographic interferometry in the presence of intense internal waves. *RENSIT: Radioelectronics. Nanosystems. Information Technology*, 2022, 14(3):279-286. DOI: 10.17725/rensit.2022.14.279.
14. Kuz'kin VM, Matvienko YuV, Pereselkov SA, Kaznacheeva ES, Tkachenko SA. Holographic method for mode selection in a shallow sea in the presence of intense internal waves. *Phys. Wave Phenom.*, 2022, 30(5):314-320.

15. Zurk LM, Rouseff D. Striation-based beamforming for active sonar with a horizontal line array. *J. Acoust. Soc. Am.*, 2012, 132(4):EL264-EL270.
16. Cockrell KL, Schmidt H. Robust passive range estimation using the waveguide invariant. *J. Acoust. Soc. Am.*, 2010, 127(5):2780-2789.
17. Bonnel J, Touze GLe, Mars JI. Physics-based time-frequency representations for underwater acoustics: Power class utilization with waveguide invariant approximation. *IEEE Signal Process. Mag.*, 2013, 30(6):120-129.
18. Emmetiere R, Bonnel J, Cristol X, Gehant M, Chonavel T. Passive source depth discrimination in deep-water. *IEEE J. of Selected Topics in Signal Processing*, 2019, 13(1):185-197.
19. Brekhovskikh LM, Lysanov YUP. *Theoretical Foundations of Ocean Acoustics*. Moscow, Nauka Publ., 2007, 370 p.
20. Kaznacheev IV, Kuz'kin VM, Kutsov MV, Lyakhov GA, Pereselkov SA. Interferometry in acoustic-data processing using extended antennas. Space-time analogy. *Phys. Wave Phenom.*, 2020, 28(4):326-332.
21. Kuz'kin VM, Matvienko YuV, Pereselkov SA, Kaznacheeva ES. Interferometric processing using a vertical linear antenna. *Vestn. MSU. Series: Physics. Mathematics*, 2020, 2:14-23.